

Determination of magnetic vortex chirality using lateral spin-valve geometry

T. Kimura^{a)} and Y. Otani

Institute for Solid State Physics, University of Tokyo, 5-1-5 Kashiwanoha, Kashiwa, Chiba 277-8581, Japan, Rikagaku Kenkyusho (RIKEN), Frontier Research System (FRS), 2-1 Hirosawa, Wako, Saitama 351-0198, Japan and Core Research for Evolutional Science and Technology (CREST), Japan Science and Technology Corporation (JST), Honcho 4-1-8, Kawaguchi, Saitama, 332-0012, Japan

J. Hamrle

Rikagaku Kenkyusho (RIKEN), Frontier Research System (FRS), 2-1 Hirosawa, Wako, Saitama 351-0198, Japan and Core Research for Evolutional Science and Technology (CREST), Japan Science and Technology Corporation (JST), Honcho 4-1-8, Kawaguchi, Saitama, 332-0012, Japan

(Received 4 May 2005; accepted 9 September 2005; published online 19 October 2005)

We demonstrate the determination of the vortex chirality using a nonlocal spin-valve measurement technique in a lateral spin valve consisting of a Permalloy (Py) disk 1 μm in diameter and a Py wire 100 nm in width. The vortex chirality is determined under two probe configurations; the disk as the current probe and the disk as the voltage probe. The vortex chirality is found to depend on the probe configuration because of the current-induced Oersted field. © 2005 American Institute of Physics. [DOI: 10.1063/1.2120911]

The recent developments in nanofabrication techniques have renewed the interest in the properties of mesoscopic-sized patterned magnetic structures. Promising application includes high-density magnetic recording media. Such patterned magnetic nanostructures show interesting behaviors because of the geometrically induced magnetostatic interactions. For example, in a ferromagnetic disk with a diameter of about a micrometer, the magnetic configuration becomes a vortex, in which the magnetization rotates around the central axis.¹ At the center of the vortex structure, the magnetization stands normal to the disk plane. The prospective usage of vortex states for data storage is accounted for by the absence of magnetostatic interaction between adjacent bits, which may extend a limit of magnetic recording densities. The stability of a magnetic vortex state² and the transition between the vortex and the single-domain states have been investigated intensively by the magneto-optic Kerr effect^{3,4} (MOKE) and magnetic force microscopy (MFM).⁵ Moreover, the behaviors of the vortex and the core provide unique fundamental properties such as Bloch point reversal.⁶ However, it has been difficult to develop techniques to study an individual disk at low temperatures. Several techniques such as micro-Hall magnetometry,⁷ microsuperconducting quantum interference device,⁸ and spin-polarized scanning tunneling microscopy⁹ have been employed for the detailed study of the vortex confined in the individual magnetic disk.

To define the magnetic vortex structure, there are two important topological quantities: the polarity and the chirality.¹⁰ The polarity, the magnetization direction of the core, can be observed by means of MFM. The chirality of the magnetic vortex is the rotational direction of the whirling magnetic moments with two degenerated states of the clockwise (CW) and counterclockwise (CCW) directions. However, none of the above-mentioned techniques can determine the chirality. Although Lorentz microscopy is a powerful means for determining the chirality of the vortex,¹¹ the com-

plex experimental conditions such as temperatures and sample thickness have to be satisfied. Here we demonstrate a relatively simple way to check the magnetic vortex chirality using lateral spin-valve geometry. This method can be applied for studying the magnetic structure of the individual magnetic disk.

A lateral spin valve used for the present study was fabricated by means of electron-beam lithography and lift-off techniques. Figure 1(a) shows a scanning-electron-microscope (SEM) image for a typical device. First we fabricated a Permalloy (Py) wire 100 nm in width and a Py disk 1 μm in diameter. Both the Py wire and the disk 30 nm in thickness were grown using an electron-beam evaporator with a base pressure of 2×10^{-9} Torr. Then, the Cu cross connecting the disk to the wire was fabricated using the lithographer followed by a resistance heating evaporation with a base pressure of 3×10^{-8} Torr. The interface between the Py and the Cu wires was well cleaned by low-voltage Ar-ion milling prior to the Cu deposition. The interface has an ohmic, very low resistive and transparent contact. The resistivities of Py and Cu wires are, respectively, 26.8 and 2.08 $\mu\Omega\text{ cm}$ at room temperature, and 18.2 and 1.04 $\mu\Omega\text{ cm}$

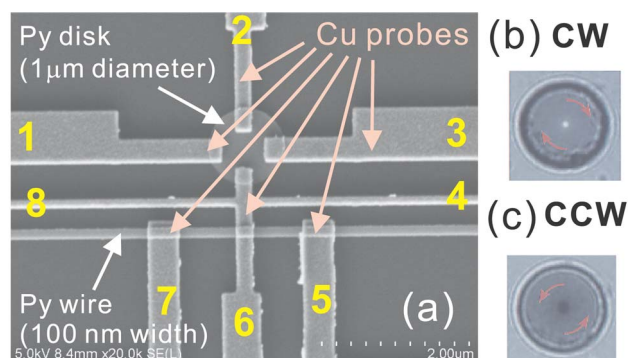


FIG. 1. (Color online) (a) Scanning-electron-microscope image of the fabricated lateral spin valve consisting of a Py disk and a Py wire. Lorentz microscope images with the chiralities of (b) CW and (c) CCW.

^{a)}Electronic mail: kimura@issp.u-tokyo.ac.jp

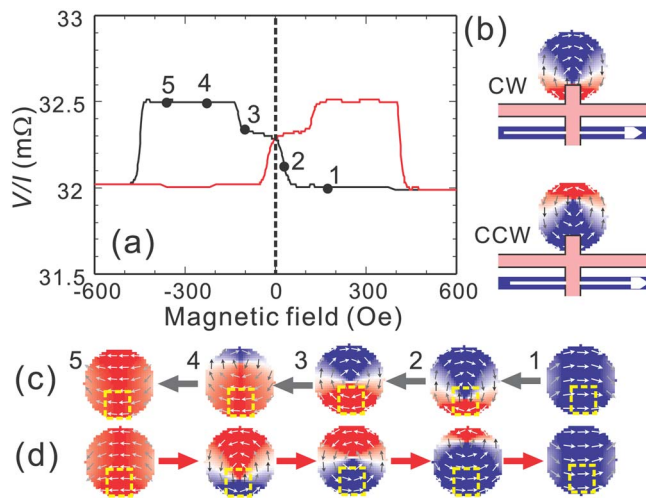


FIG. 2. (Color online) (a) Nonlocal spin-valve signals measured with the current probes 1 and 8 and the voltage probe 4 and 5 measured at 4.1 K. The magnetization configurations of the disk (b) in the negative sweep and (c) in the positive sweep expected from the NLSV signal.

at 4 K. The magnetoresistance measurement was performed by using conventional current-bias lock-in technique with the amplitude of 0.5 mA. The external magnetic field H was applied along the wire. Separately performed Lorentz microscopy also confirmed that the domain structure of the Py disk with the same dimension as that in the spin valve is vortex as shown in Figs. 1(b) and 1(c).

In the ferromagnetic disk, the magnetization reversal is known to proceed through the nucleation, displacement, and annihilation of the vortex.³ We employ the current probes 1 and 8 and the voltage probes 4 and 5 for the nonlocal spin-valve (NLSV) measurement. Here, we use the disk and the wire as the injector and detector, respectively. In this configuration, the spin signal is proportional to $\cos^2 \theta/2$ with the angle θ between the Py wire and the local magnetization in the Py disk beneath the injecting probe.¹² As shown in Fig. 2(a), the NLSV loop exhibits a clear spin-valve signal. The observed signal is symmetric with respect to H . The signal varies stepwise. The first step appears in the vicinity of the zero field, followed by a sudden resistance rise at around the field of -100 Oe, and finally by the large jump at about -400 Oe in association with the magnetization reversal of the Py wire. The first and second abrupt steps in low magnetic fields, respectively, correspond to the nucleation of the vortex within the region beneath the injecting probe and the vortex escaping from the injecting region. The vortex nucleation point depends on the chirality. The vortex nucleates from the bottom edge for the CW or the top edge for the CCW as in Fig. 2(b). Therefore, when the chirality is the CW, the spin signal increases as the vortex nucleates from the bottom edge of the disk. On the other hand, when the chirality is CCW, the signal cannot change with the vortex nucleation. Since the first abrupt step in the negative sweep occurs at the field around 50 Oe, the chirality should be the CW as in Fig. 2(c). After nucleation, the vortex moves perpendicular to the magnetic field, and the vortex reaches the center at the zero field. In that case, the spin signal should gradually increase to the value corresponding to the antiparallel state. However, the observed spin signal shows only a tiny increase in the field range from 0 to -100 Oe. As will be discussed later, this may be because the vortex is trapped at the junction.

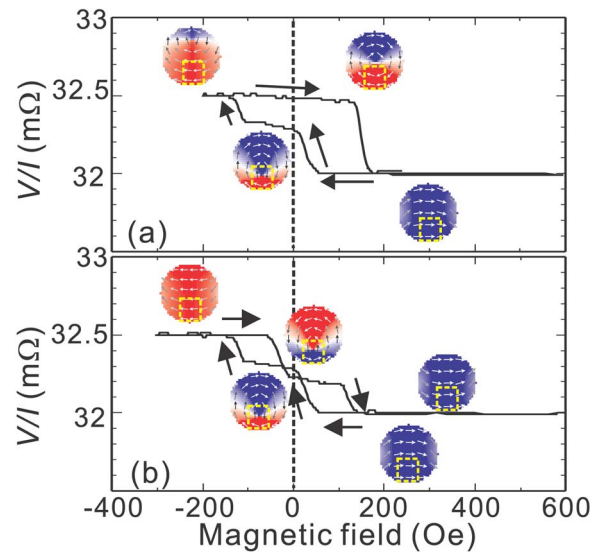


FIG. 3. (Color online) Minor loops of the NLSV signal with the domain structure of the disk (a) in the field range from 600 to -200 Oe and (b) from 600 to -300 Oe.

tion because of the current-induced Oersted field. When the magnetic field reaches the field around -100 Oe, the second abrupt change occurs owing to the vortex escaping from the injecting region. Since the obtained spin signal of each sweep is symmetric with respect to the magnetic field, the vortex nucleates from the bottom of the disk also in the positive sweep. In this case, the chirality of the vortex is CCW as shown in Fig. 2(d). These results mean that the vortex chirality alternates in the sweep direction.

To confirm the above result, we then measured the minor loops. Figure 3(a) shows a minor loop measured in the field range from 600 to -200 Oe. After the sweep direction is changed, the spin signal shows a small decrease followed by a large step at the field of 150 Oe. As will discuss later, the vortex displacement is affected by the current-induced field also in this case. The small decrease corresponds to the small displacement of the vortex from the top to the center. The abrupt resistance change in the positive sweep is caused by the annihilation of the vortex. We expect that, in this minor loop, the vortex escapes from the injecting region at the field of -200 Oe, but is not swept out of the disk. Therefore, the chirality of the vortex remains CW even in the positive sweep. Figure 3(b) shows the minor loop in the field range from 600 to -300 Oe. The signal in the positive sweep has two abrupt changes unlike Fig. 3(a). We can understand that the two abrupt changes in the positive sweep are due to the vortex nucleation and the escape from the injecting region as in the negative sweep. The vortex annihilates from the disk at the field of 300 Oe, and nucleates from the bottom again at the field of -50 Oe. This means that the chirality of the vortex alternates in the sweep direction.

We also measured the NLSV signal using the current probes 4 and 5 and the voltage probes 1 and 8. In this probe configuration, the disk was used as a detector for the spin accumulation in the Cu probe. The signal also exhibits clear spin accumulation effect as shown in Fig. 4(a), but is rather different from Fig. 2(a). Especially, the signal change is asymmetric with respect to the magnetic field. The signal in the negative sweep shows the close values in the antiparallel state at zero field and reaches the antiparallel state rapidly.

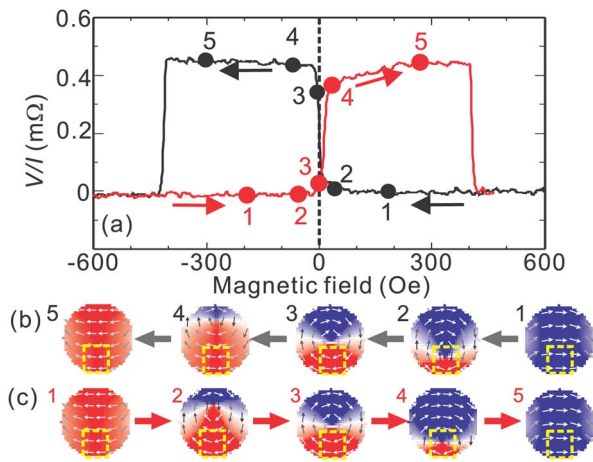


FIG. 4. (Color online) (a) Nonlocal spin-valve signals with the current probes 4 and 5 and the voltage probes 1 and 8 measured at 4.1 K. The magnetization configurations of the disk and the wire (b) in the negative sweep and (c) in the positive sweep expected from the NLSV signal.

This means that the vortex nucleates and then escapes from the detecting region as shown in Fig. 4(b). On the other hand, in the positive sweep, the signal shows the close values in the parallel state at zero field and shows gradual change up to 300 Oe. From these results, it is inferred that the vortex nucleates from the top edge and penetrates into the detecting region as shown in Fig. 4(c). Thus, in this probe configuration, the vortex chirality remains CW during the measurement.

We here discuss why the chirality depends on the probe configuration. The most important difference between two configurations is whether the current flows through the disk or not. When the disk is used as the injector, the current flows across the interface between the Py disk and the Cu cross. Such a current flow induces the rotational magnetic field around the junction due to Ampere's law, and assists the nucleation of the vortex from the junction. The rotational direction of the induced field depends on the polarity of the current. Since the current for the present measurement is alternating, both CW and CCW rotational fields are induced. However, as shown in Fig. 5(a), one of the two rotational magnetic fields is more effective than the other for nucleating the vortex from the injecting region because of the better magnetostatic coupling between the magnetization in the disk and the rotational field. The other one therefore does not contribute to the vortex nucleation. In this way, the current flowing through the disk assists the vortex to nucleate from the injecting region. The induced rotational field also affects the displacement of the vortex. According to the typical magnetization process of the magnetic disk, after the nucleation of the vortex, the vortex moves gradually to the edge of the opposite side. However, as in Fig. 2(a), we did not observe the resistance change corresponding to such a vortex dis-

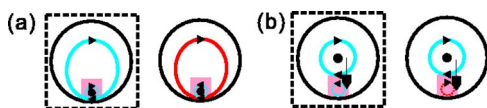


FIG. 5. (Color online) Schematic illustrations of the current-induced Oersted field with the magnetization configurations around (a) the field of the vortex nucleation and (b) that of the vortex displacement from the center to the bottom edge. The illustration enclosed by the dotted line is effective for each case.

placement. After the vortex nucleation, a small gradual resistance increase and the second abrupt change at the field of -100 Oe were observed. As in Fig. 5(a), the induced rotational field causes the magnetostatic coupling, leading to trapping the vortex at the junction. Therefore, the vortex displacement from the junction is probably prevented by the induced field. The abrupt resistance change at the field of -100 Oe may correspond to the deeping of the vortex from the junction. The NLSV signal change for the positive sweep in Fig. 3(a) also can be explained by considering the Oersted field. When the vortex moves from the center into the junction, the one rotational field causes better magnetostatic coupling than that in the other one. Such an Oersted field prevents the vortex from entering the junction, as in Fig. 5(b). Therefore, the NLSV signal in the positive sweep of Fig. 3(a) did not show the gradual change. The vortex enters into the junction and then annihilates immediately. This process corresponds to the abrupt signal change at the field of 150 Oe. On the other hand, when the disk is used as the detecting probe, there is no current flowing into the disk, wherein both CW and CCW states are degenerated.¹³ A possible reason why the chirality remains the same direction during the measurement is that the magnetization of the disk is not fully aligned with the magnetic field and still forms a C-shape state in the maximum applied field of 600 Oe.¹⁴

In conclusion, we fabricated a lateral spin valve consisting of a Py disk $1 \mu\text{m}$ in diameter and a Py wire 100 nm in width and demonstrated that the chirality of the vortex can be determined by the NLSV measurement. The vortex chirality is found to depend on the probe configuration because the current flowing through the disk facilitates the vortex nucleation at the current-injecting junction. The NLSV measurement, with a disk used as a voltage probe, may be useful for the detailed study on the magnetization process of the individual disk.

The authors would like to thank Dr. Y. Togawa, Dr. K. Harada, and Dr. T. Matsuda in Quantum phenomena observation technology laboratory of RIKEN FRS for the observation of Lorentz microscopy. Technical support from the Nanoscience Development and Support Team of RIKEN is gratefully acknowledged.

¹T. Shinjo, T. Okuno, R. Hassdorf, K. Shigeto, and T. Ono, *Science* **289**, 930 (2000).

²N. Kikuchi, S. Okamoto, O. Kitakami, Y. Shimada, S. G. Kim, Y. Otani, and K. Fukamichi, *J. Appl. Phys.* **90**, 6548 (2001).

³R. P. Cowburn, D. K. Koltsov, A. O. Adeyeye, M. E. Welland, and D. M. Tricker, *Phys. Rev. Lett.* **83**, 1042 (1999).

⁴Y. Otani, H. Shima, K. Guslienko, V. Novosad, and K. Fukamichi, *Phys. Status Solidi A* **189**, 521 (2002).

⁵T. Okuno, K. Shigeto, T. Ono, K. Mibu, and T. Shinjo, *J. Magn. Magn. Mater.* **240**, 1 (2002).

⁶A. Thiaville, J. M. Garcia, R. Dittrich, J. Miltat, and T. Schrefl, *Phys. Rev. B* **67**, 094410 (2003).

⁷M. Rahm, M. Schneider, J. Biberger, R. Pulwey, J. Zweck, D. Weiss, and V. Umansky, *Appl. Phys. Lett.* **82**, 4110 (2003).

⁸W. Wernsdorfer, K. Hasselbach, D. Mailly, B. Barbara, A. Benoit, L. Thomas, and G. Suran, *J. Magn. Magn. Mater.* **145**, 33 (1995).

⁹A. Wachowiak, J. Wiebe, M. Bode, O. Pietzsch, M. Morgenstern, and R. Wiesendanger, *Science* **298**, 577 (2002).

¹⁰J. Shibata, K. Shigeto, and Y. Otani, *Phys. Rev. B* **67**, 224404 (2003).

¹¹M. Schneider, H. Hoffmann, and J. Zweck, *Appl. Phys. Lett.* **77**, 2909 (2000).

¹²T. Kimura, J. Hamrle, and Y. Otani (unpublished).

¹³S. Savel'ev and F. Nori, *Phys. Rev. B* **70**, 214415 (2004).

¹⁴K. Yu. Guslienko, V. Novosad, Y. Otani, H. Shima, and K. Fukamichi, *Phys. Rev. B* **65**, 024414 (2002).